Computational architecture for full-color holographic displays based on anisotropic leaky-mode modulators

Sundeep Jolly[1], Daniel Smalley[2], James Barabas[1], and V. Michael Bove, Jr.[1]

[1] Media Laboratory, Massachusetts Institute of Technology, 77 Massachusetts Avenue, Rm. E15-444, Cambridge, MA, 02139, United States of America

[2]Department of Electrical and Computer Engineering, Brigham Young University, Provo, UT, 84602, United States of America

ABSTRACT

The MIT Mark IV holographic display system employs a novel anisotropic leaky-mode spatial light modulator that allows for the simultaneous and superimposed modulation of red, green, and blue light via wavelength-division multiplexing. This WDM-based scheme for full-color display requires that incoming video signals containing holographic fringe information are comprised of non-overlapping spectral bands that fall within the available 200 MHz output bandwidth of commercial GPUs. These bands correspond to independent color channels in the display output and are appropriately band-limited and centered to match the multiplexed passbands and center frequencies in the frequency response of the mode-coupling device. The computational architecture presented in this paper involves the computation of holographic fringe patterns for each color channel and their summation in generating a single video signal for input to the display. In composite, 18 such input signals, each containing holographic fringe information for 26 horizontal-parallax only holographic lines, are generated via three dual-head GPUs for a total of 468 holographic lines in the display output. We present a general scheme for full-color CGH computation for input to Mark IV and furthermore depict the adaptation of the diffraction specific coherent panoramagram approach to fringe computation for the Mark IV architecture.

Keywords: dynamic holographic displays, computational display holography, acousto-optic modulation, integrated optics, single-sideband modulation, wavelength-division multiplexing, GPU computation

1. INTRODUCTION

Holographic display architectures have typically relied on space-division[1,2] or time-division[3] multiplexing techniques in order to achieve full-color imagery. Although such methods can provide for compelling color holographic imagery, they often require cumbersome optical geometries or diffraction-correcting elements in order to ensure the proper overlap of holographic reconstructions from each of the red, green, and blue color channels. Furthermore, space-division or time-division multiplexing techniques reduce the overall effective bandwidth available for modulation of light by fringe patterns and thereby limit achievable frame rates and/or image sizes.

The MIT Mark IV holographic video system is a proof-of-concept system for horizontal-parallax only holographic display based upon a novel anisotropic leaky-mode acousto-optic light modulator implemented as a $LiNbO_3$ guided-wave device. This light modulator offers significant advantages for holographic video displays, including high deflection angle due to near-collinear incidence of unmodulated light on acoustic gratings, polarization rotation of diffracted light for noise extraction, and the capacity for wavelength-division multiplexing for full-color displays.[4] Unlike conventional bulk-wave acousto-optic devices, anisotropic leaky-mode devices rely upon surface acoustic wave phenomena and therefore tight placement of multiple independent channels is possible. This enables an extremely high space-bandwidth product; we have demonstrated fabrication of modulators with up to 2500 adjacent channels on a single substrate.

Unlike space-division or time-division multiplexing schemes for the generation of full-color holographic imagery, the wavelength-division multiplexing scheme of the Mark IV display requires the generation of a single analog signal (per channel) containing holographic fringe information for all independent color channels in a frequency-division multiplexed manner. We have previously demonstrated the display of single-view holographic stereograms as a validation of the Mark

Corresponding Author: sjolly@media.mit.edu

IV operating principles and display geometry. In this paper, we review the MIT Mark IV holographic video display and its full-color operating principle, review techniques for fringe pattern generation, and depict progress in algorithm development and implementation for display of full-color, three-dimensional holographic images.

2. MIT MARK IV HOLOGRAPHIC VIDEO SYSTEM

2.1 Anisotropic Leaky-Mode Spatial Light Modulator

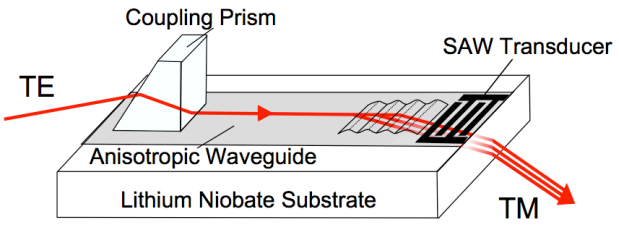

Figure 1. Light coupling, guided-to-leaky mode conversion, and light modulation via acousto-optic Bragg-regime diffraction in a single-channel anisotropic leaky-mode device implemented as guided-wave device on a $LiNbO_3$ substrate.

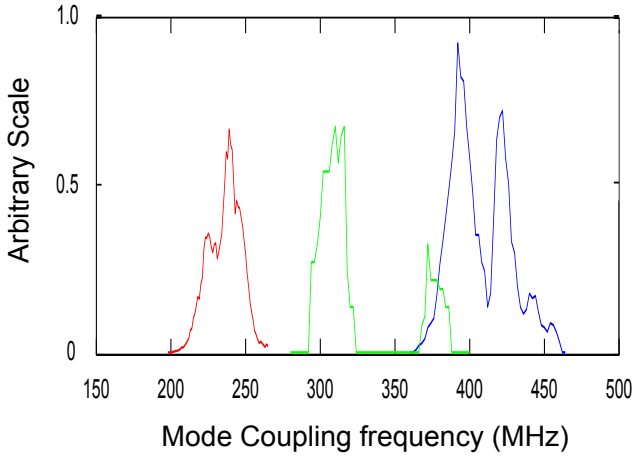

Figure 2. Typical mode-coupling frequency response of an anisotropic leaky-mode modulator, depicting nearly non-overlapping acoustic spectral bands that act exculsively and independently upon different wavelengths of guided light. The left-most band corresponds to mode conversion and Bragg-regime diffraction of red light, while the center and right-most bands correspond to that for green and blue light, respectively.

The Mark IV holographic video display is built around a one-dimensional anisotropic leaky-mode spatial light modulator, implemented as a guided-wave device on a $LiNbO_3$ substrate. Fig. 1 depicts the structure and function of a single-channel anisotropic leaky-mode modulator. In this modulator, laser light of a particular linear polarization is coupled into an anisotropic waveguide via the use of a coupling prism, at which point the coupled light becomes a guided mode. A surface acoustic wave (SAW) transducer is patterned at one end of the device; when this transducer is excited by an RF signal containing holographic fringe information, it launches a surface acoustic wave along the waveguide. The guided laser light is incident upon this surface acoustic wave at a nearly collinear angle and experiences Bragg-regime acousto-optic diffraction in accordance with the spatial frequencies present in the acoustic grating. Because of device characteristics,[5] the diffracted light is mode-converted into a leaky mode of an orthogonal polarization and exits the waveguide. Our current devices employed for spatial light modulation employ multiple independent channels, each comprised of an anisotropic waveguide and a SAW transducer. Each independent channel requires its own RF input signal to the SAW transducer. Details on the fabrication process of anisotropic leaky-mode modulator devices have been previously published.[4,6] Mark IV uses an 18-channel modulator.

With appropriate fabrication parameters, anisotropic leaky-mode modulators can be made to allow for the simultaneous and superimposed modulation of red, green, and blue light in a wavelength-division multiplexed fashion. A typical mode-coupling acoustic frequency response from such a modulator is shown in Fig. 2 and depicts nearly non-overlapping acoustic spectral bands that act independently and exclusively upon different wavelengths of incoming light, with the band acting exclusively upon red light at the lower end of the acoustic spectrum followed by those acting upon green and blue at higher acoustic frequency ranges.

One possible interpretation of the depicted mode-coupling frequency response of an anisotropic leaky-mode modulator entails that the lower and upper cutoff frequencies per acoustic spectral band correspond to the minimal (i.e., zero) and

maximal deflection angles for the given mode-coupled frequency. It is therefore convenient to interpret the requisite RF excitation as a frequency-division multiplexed signal comprised of single-sideband modulated spectral bands, each corresponding to an appropriately up-converted and bandlimited holographic signal for a particular color channel.

2.2 Display Geometry and Supporting Electronic Architecture

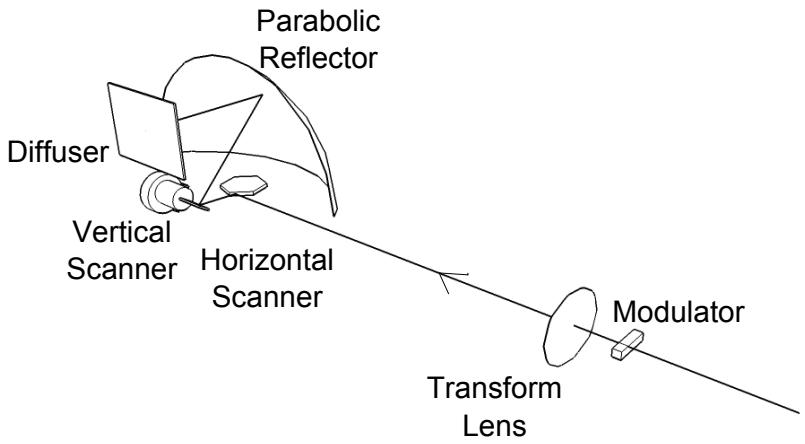

Figure 3. Modified Scophony optical geometry employed in the MIT Mark IV holographic display system.

The supporting optical geometry of the Mark IV display[7] (depicted in Fig. 3) is a modification of that employed in the Scophony acousto-optic mechanical television system[8] and closely parallels that of the first-generation MIT holographic video display, the Mark I.[9] The multi-channel, full-color output of the anisotropic leaky-mode modulator is incident upon a Fourier-transforming lens, whose Fourier plane coincides with a polygonal scanner used for de-scanning of the propagating SAW grating. A galvanometric scanner is used to vertically multiplex several holographic lines to raster a complete holographic image within the persistence time of the human eye. A parabolic reflecting mirror acts as the output lens of a telescope and is used to form the holographic reconstruction onto a vertical diffuser.

GPU-based computation is used to generate the holographic fringe patterns that drive the SAW transducers. Fig. 4 depicts the function of supporting electronics that are used within Mark IV to generate appropriate drive signals for the horizontal and vertical scanning elements as well as condition the GPU-generated holographic information for SAW-transducer input. Because the acousto-optic mode coupling frequency response requires that SAW excitation occurs at RF frequencies approximately contained within the 200 MHz to 400 MHz range, the (available) 200 MHz analog baseband signal generated via a GPU must be appropriately up-converted and amplified to that frequency range. The horizontal sync signal generated by the GPU is used to phase-lock the horizontal scanner (driven by a square pulse signal) for appropriate de-scanning of the propagating SAW grating. Likewise, the vertical sync signal from the GPU is used in tandem with a divided-down horizontal sync signal for phase-locking of the vertical scanner (driven by a sawtooth signal) for appropriate time-multiplexing of the aggregate holographic reconstruction. Mark IV currently employs 26 discrete vertical steps per horizontal sync pulse; this translates directly into 26 horizontal-parallax only holographic lines per device channel. Viewed in aggregate, Mark IV is capable of delivering 468 total holographic lines in its display output.

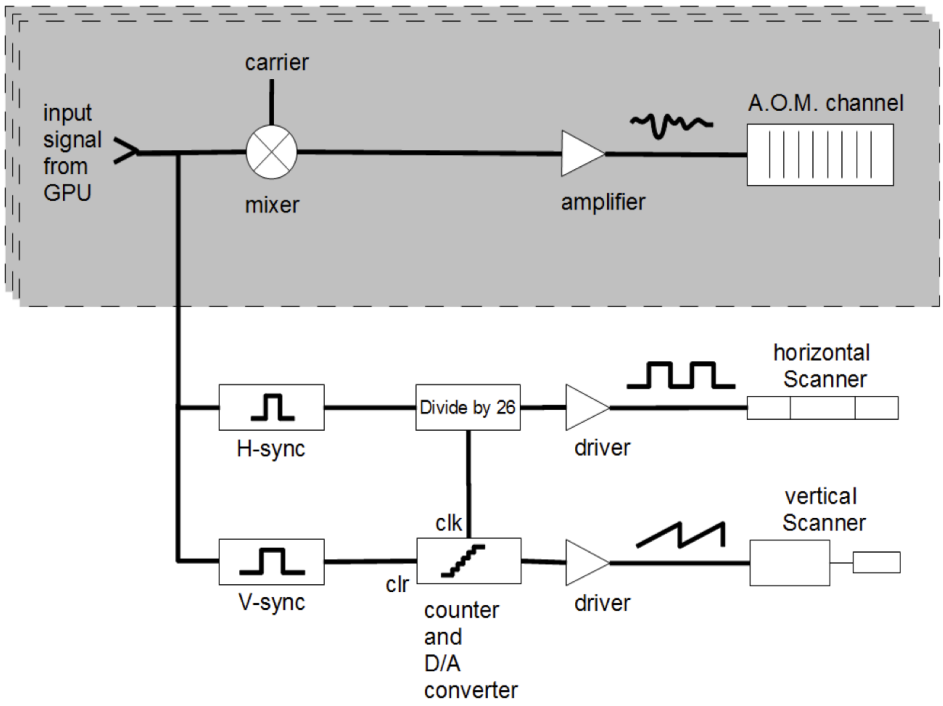

Figure 4. Electrical subsystem for conditioning of GPU-generated fringe information for SAW-transducer input and control of timing of both horizontal and vertical scanners.

3. COMPUTATIONAL METHODS

Simultaneous and superimposed modulation of red, green, and blue light is accomplished via a frequency-division multiplexing scheme, in which three non-overlapping, multiplexed Fourier-domain sidebands contain the holographic fringe information corresponding to each color channel. This approach requires the generation of single-sideband modulated fringe patterns per color and their Fourier-domain multiplexing in forming a analog signal appropriate for input to the Mark IV electronic subsystem. The current iteration of the Mark IV electronics does not directly handle single-sideband modulation of color channel information and therefore fringe computation for all three color channels, single-sideband modulation, and frequency-division multiplexing are handled via GPU computation. We will begin detailing methods for multiplexed signal generation for the general case of a full-color computer-generated hologram and proceed to discuss the specific case of diffraction-specific stereogram algorithms, which have been used in previous MIT holographic displays for efficient video-rate computation of fringe patterns.

3.1 Single-Sideband Modulation for a Full-Color General CGH

Given a mode-coupling frequency response of the type depicted in Fig. 2, it is necessary that holographic fringe information per color channel is appropriately band-limited and translated in frequency to match the multiplexed passbands. We will note that in this context, "band-limited" refers to a computed holographic fringe pattern in which spatial frequencies above a certain threshold (corresponding to the bandwidth of a color passband in the mode-coupling frequency response) are rejected or otherwise not computed. Assuming that this criterion is met during the computation of a general (Fresnel or other interference-based) CGH for display on Mark IV, the requisite analog signal for input to the electronic subsystem is formed via single-sideband modulation per color channel and frequency-division multiplexing. The overall process is depicted in Fig. 5.

For a one-dimensional fringe pattern $t(x)$, the single-sideband modulated form $t_{ssb}(x)$ with carrier frequency f_0 is given by

$$t_{ssb}(x) = t(x)\cos(2\pi f_0 x) - \mathcal{H}\{t(x)\}\sin(2\pi f_0 x) \tag{1}$$

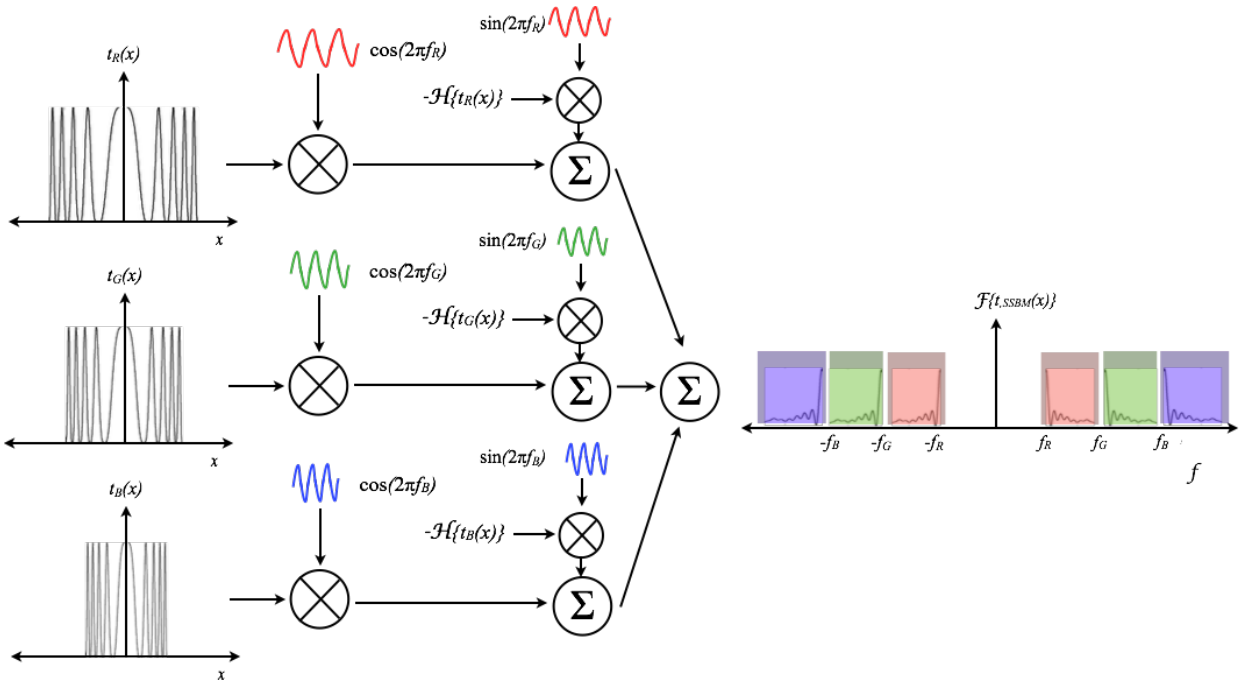

Figure 5. Depiction of single-sideband modulation process and frequency-division multiplexing scheme for generation of appropriate signal for input to Mark IV electronics in the case of a general Fresnel CGH.

where $\mathcal{H}$ denotes Hilbert transformation.[10] The Hilbert transform $\mathcal{H}\{t(x)\}$ is defined as

$$\mathcal{H}\{t(x)\} = \frac{1}{\pi}\,\mathrm{p.v.}\int_{-\infty}^{\infty}\frac{t(x')}{x-x'}dx' \tag{2}$$

where p.v. denotes the Cauchy principal value.[11] Note that Eq. 2 can be expressed as a convolution of the signal $t(x)$ with the kernel $1/\pi x$. Because of numerical issues associated with directly computing the integral in Eq. 2, software-based implementation of single-sideband modulation is often accomplished via a Fourier-domain method in which the Hilbert transform operator $\sigma_H = \mathcal{F}\{1/\pi x\} = j\mathrm{sgn}(2\pi f)$ (where sgn is the Signum function) is multiplicative upon the Fourier transform of $t(x)$. Therefore,

$$\mathcal{F}\left[\mathcal{H}\{t(x)\}\right] = j\mathrm{sgn}(2\pi f)\mathcal{F}\{t(x)\} \tag{3}$$

where $\mathcal{F}$ denotes Fourier transformation and

$$t_{SSB}(x) = t(x)\cos(2\pi f_0 x) - \mathcal{F}^{-1}\left[j\mathrm{sgn}(2\pi f)\mathcal{F}\{t(x)\}\right]\sin(2\pi f_0 x) \tag{4}$$

where $\mathcal{F}^{-1}$ denotes inverse Fourier transformation. This modulation scheme is amenable to software implementation via the Fast Fourier transform.

For computed fringe patterns corresponding to red, green, and blue color channels (e.g., $t_R(x)$, $t_G(x)$, and $t_B(x)$, as shown on the left side of Fig. 5), single-sideband modulation with carrier frequencies corresponding to the lower cutoff frequencies of the color passbands in the mode-coupling device frequency response (e.g., f_R, f_G, and f_B) produces the correctly translated passbands (e.g., $t_{SSB,R}(x)$, $t_{SSB,G}(x)$, and $t_{SSB,B}(x)$). Summation of these three single-sideband modulated fringe patterns as $t_{FDM}(x) = t_{SSB,R}(x) + t_{SSB,G}(x) + t_{SSB,B}(x)$ then produces the composite, frequency-division multiplexed fringe signal for input to the electronic subsystem, as shown on the right side of Fig. 5.

3.2 Single-Sideband Modulation for a Full-Color Diffraction-Specific Coherent Panoramagram

The approach to frequency-division multiplexed fringe signal generation depicted in Section 3.1, while amenable to software implementation, is computationally expensive due to the two Fourier transformation steps involved in computation of the Hilbert transform. In the case of display of a Fresnel (or other physically-based) CGH, this approach is necessary due to the superposition of spatial frequencies at each hologram point. However, in the case of a diffraction-specific stereogram, single-sideband modulation can be achieved in a more computationally efficient manner.

Diffraction-specific stereogram approaches to hologram computation employ hologram discretization in space and spectrum, commonly utilizing holographic elements (or hogels) as primitives. Such a primitive is an analytical or pre-computed 1-D chirped grating (or 2-D Fresnel zone plate, in the case of full-parallax) that is modulated with view information corresponding to the luminance of a scene over the angle space; a fully-populated light field representation of a scene is therefore readily converted to a diffraction-specific holographic stereogram.

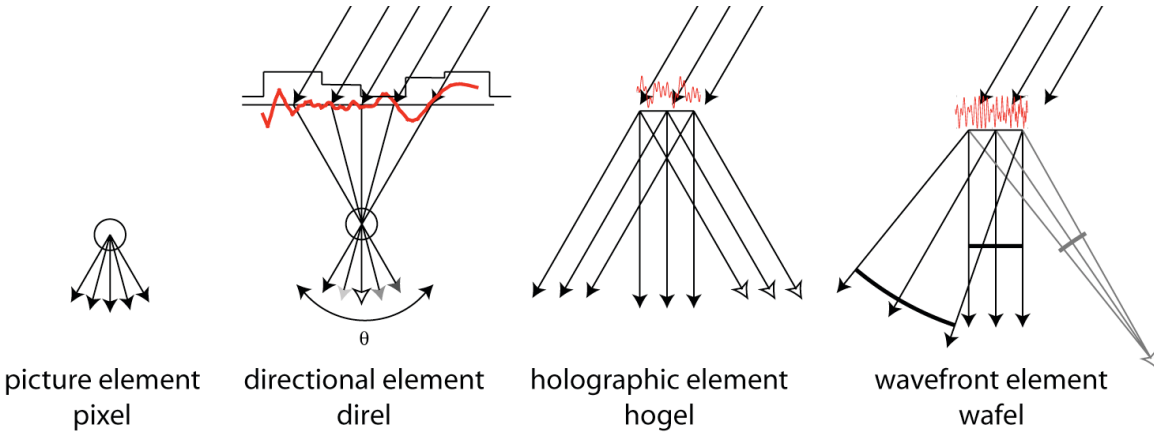

Figure 6. Comparative affordances of the pixel, direl, hogel, and wafel.

We have previously introduced the *diffraction-specific coherent panoramagram*, which is a diffraction-specific approach to multi-view holographic stereogram generation that retains a higher degree of the wavefront curvature of a given 3-D scene.[12] The algorithm uses scene depth information, either from a synthetic graphics model or captured via a rangefinding camera,[13] to select appropriately chirped holographic gratings for modulation with scene luminance information. Such an approach generates wavefront element primitives, or wafels. The comparative affordances of the wafel relative to those of the pixel, direl, and hogel are depicted in Fig. 6. Relative to conventional holographic elements (hogels) which are limited to producing planar wave curvature with intensity variation per view direction, wafels can produce a higher degree of wavefront curvature per view direction.

Following our earlier derivation,[12] the equation specifying the transmittance function $t(x)$ of an unmodulated, chirped holographic grating defining a wafel is

$$t(x) = \cos\left[\frac{2\pi}{\lambda}\left(\sqrt{(x-x_0)^2+z_0^2} - x_0 + x\sin\theta_r\right)\right] \tag{5}$$

where x is the position on the composite hologram transmittance function, (x_0, z_0) is the position of a scene point to be reconstructed, and θ_r is the angle of the reconstruction beam relative to the normal of the hologram plane. Examination of this function reveals that the square root term produces a chirped frequency distribution along x whose chirp rate $\partial f/\partial x$ depends on z_0, the x_0 term produces a phase shift such that $t(x)$ has zero phase at $x = x_0$, and that the $x\sin\theta_r$ term produces a constant frequency dependent on the angle of the reconstruction beam θ_r.

Because the holographic grating is defined by a single cosine functional composition, translating the positive and negative halves of the frequency spectrum by $\pm f_0$ can be accomplished by the addition of an $x\lambda f_0$ term in the cosine argument.

The single-sideband modulated form of the chirped grating is then

$$t_{SSB}(x) = \cos\left[\frac{2\pi}{\lambda}\left(\sqrt{(x-x_0)^2+z_0^2} - x_0 + x(\sin\theta_r + \lambda f_0)\right)\right] \tag{6}$$

A derivation of Eq. (6) can be found in Appendix A.

Computation of the overall wafel proceeds in the normal diffraction-specific fashion, with the wafel's transmittance computed as the multiplication of the single-sideband chirped grating $t_{SSB}(x)$ with a view modulation function $m(x)$. A full-color, frequency-division multiplexed wafel for is computed via a summation as $t_{FDM}(x) = m_R(x) \cdot t_{SSB,R}(x) + m_G(x) \cdot t_{SSB,G}(x) + m_B(x) \cdot t_{SSB,B}(x)$, where $t_{SSB,R}(x)$, $t_{SSB,G}(x)$, and $t_{SSB,B}(x)$ are single-sideband modulated chirped gratings computed for the appropriate illumination wavelengths λ and (as above, in the case of a general CGH) employing carrier frequencies corresponding to the lower cutoff frequencies of the color passbands in the mode-coupling device frequency response (e.g., f_R, f_G, and f_B). $m_R(x)$, $m_G(x)$, and $m_B(x)$ are view modulation functions per color. Many such frequency-division multiplexed wafels are then spatially multiplexed to form a composite holographic line.

3.3 Carrier Frequency Conversion

Note that the carrier frequency f_0 in Eqs. 4 and 6 is a *spatial* frequency, whereas the mode-coupling frequencies depicted in Fig. 2 are *temporal* frequencies. To relate a mode-coupling frequency corresponding to a color band to a spatial carrier frequency as used in the computation of Eqs. 4 and 6, information about the pixel clock rate of the GPU providing the fringe signal to the Mark IV electronic subsystem and the effective pixel dimension in the output of the display is required. Assuming a pixel clock rate P (pixels/s), N pixels per scanline in the display output, and a hologram plane width of w, the conversion relationship between a temporal frequency f_T and a spatial frequency f_0 is given as $f_0 = Nf_T/Pw$. As an example, we consider the spatial carrier frequency required to translate a given fringe spectral band by 75 MHz in the temporal frequency domain, or approximately that required for offsetting (relative to the baseband red color channel) a fringe spectral band for the green color channel in a typical modulator mode-coupling frequency response. Assuming a pixel clock rate $P = 400$ Mpixels/s (maximum typical of many commercially available GPUs), hologram plane width of $w = 300$ mm, and $N = 512800$ pixels per scanline, the spatial carrier frequency is computed to be $f_0 = 3.205$ x 10^5 m^{-1}.

3.4 Analysis

As a validation of our computational approach, we analyze single-sideband modulated chirped gratings given by Eq. 6 in frequency and space-frequency domains. Fig. 7(a) depicts the time-domain form of a baseband chirp signal generated via Eq. 5 for reconstruction of a scene point at $(x_0, z_0) = (0, 5$ x $10^{-2})$ m relative to the hologram plane origin at $(0, 0)$ and normal illumination (i.e., $\theta_r = 0°$). The power spectral density distribution in Fig. 7(b) depicts a baseband signal and the short-time Fourier transform in Fig. 7(c) depicts a linearly increasing relationship between spatial position x and spatial frequency u. Figs. 7(d) and 7(e) depict the power spectral density and short-time Fourier transform of a single-sideband modulated chirped grating with temporal carrier frequency $f_T = 75$ MHz; the spatial carrier frequency f_0 is computed employing the relationship and parameters described in the preceding text. The sidebands are appropriately translated in frequency while the STFT distribution is frequency-shifted while retaining its spatial variance, therefore numerically validating Eq. 6.

We furthermore validate the frequency-division multiplexing of three chirped gratings, with temporal carrier frequencies of $f_{T1} = 0$ MHz (baseband; no modulation), $f_{T2} = 75$ MHz, and $f_{T3} = 150$ MHz and spatial carrier frequencies computed as depicted in the preceding text. These frequencies roughly correspond to typical lower-cutoff frequencies for red, green, and blue color passbands in a mode-coupling frequency response (e.g., Fig. 2) after accounting for the 200 MHz offset performed via amplitude modulation in the Mark IV electronics. Fig. 8 depicts this result in the power spectral density and short-time Fourier transform.

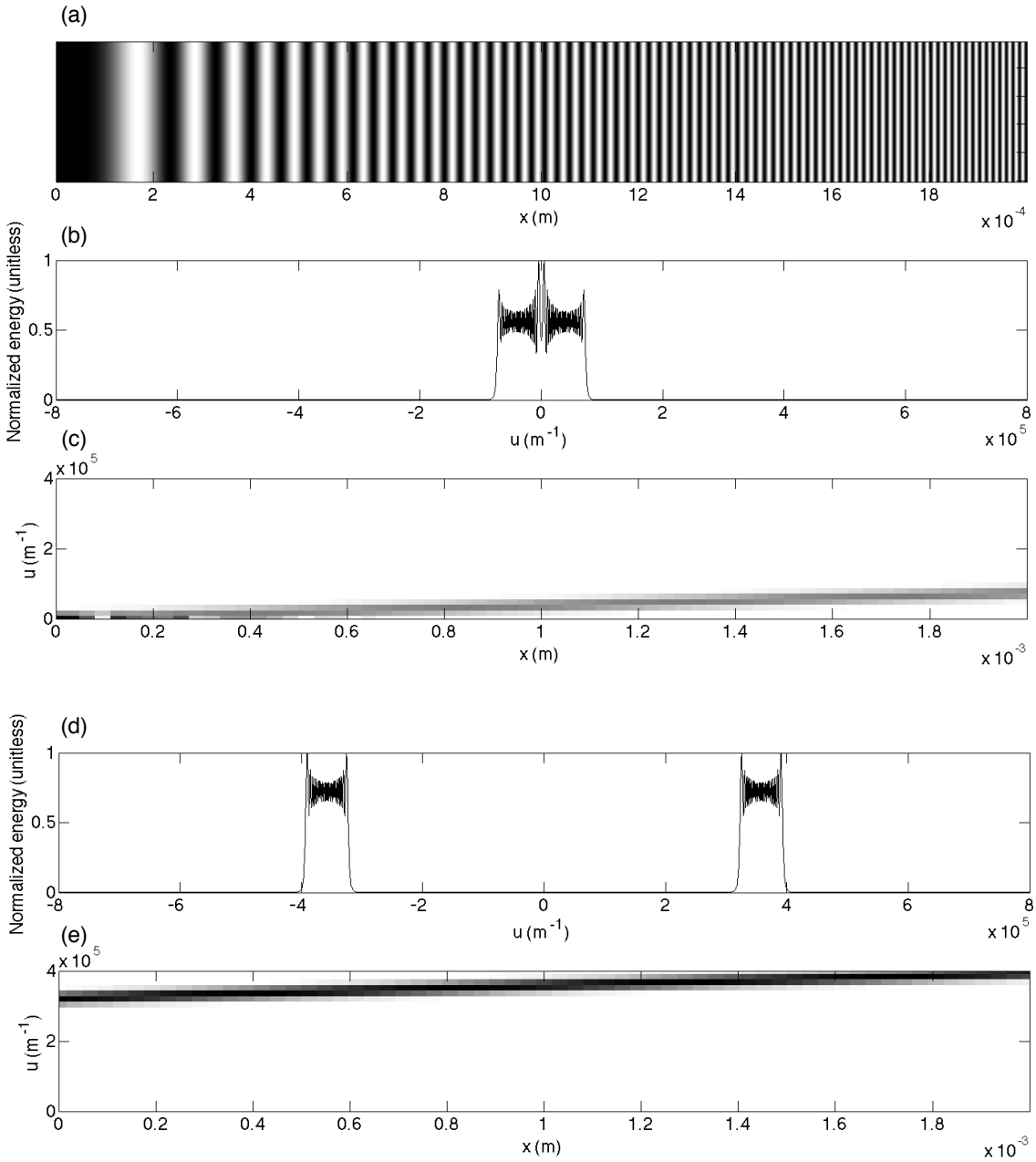

Figure 7. Effect of single-sideband modulation on a chirped transmittance function (Eqs. 5 and 6) defining a wafel aperture, given a scene point at $(x_0, z_0) = (0, 5 \text{ x } 10^{-2})$ m relative to the hologram plane origin at $(0, 0)$ and normal illumination (i.e., $\theta_r = 0°$). (a) Space-domain representation of chirped grating defined over a 2 mm aperture, (b) Normalized power spectral density distribution of chirped grating, depicting a Hermitian-symmetric baseband signal comprised of bandlimited sidebands, (c) Short-time Fourier transform of chirped grating, depicting a linear relationship between spatial position x and spatial frequency u, (d) Normalized power spectral density distribution of single-sideband modulated chirped grating with temporal carrier frequency $f_T = 75$ MHz and spatial carrier frequency calculated as $f_0 = 3.205 \text{ x } 10^5$ m^{-1}, depicting Hermitian-symmetric bandlimited sidebands translated in frequency relative to baseband, (e) Short-time Fourier transform of single-sideband chirped grating, depicting a translation in frequency relative to baseband.

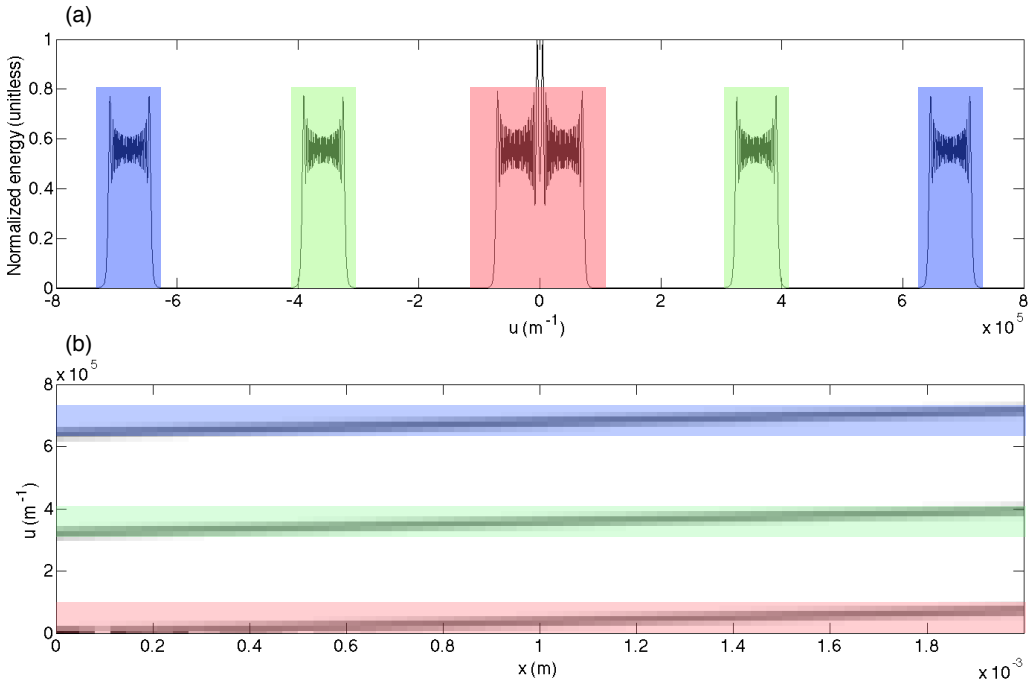

Figure 8. Effect of frequency-division multiplexing of several single-sideband modulated chirped gratings on composite signal. (a) Power spectral density distribution of frequency-division multiplexed composite fringe pattern, comprised of spectral bands matching the multi-color mode-coupling frequency response of an anisotropic leaky-mode modulator as seen in Fig. 2, (b) Short-time Fourier transform of frequency-division multiplexed fringe signal, depicting linear relationships between spatial position x and spatial frequency u and offsets in frequency for red, green, and blue chirped gratings.

4. PROJECT STATUS

Our algorithm for full-color holographic fringe signal generation via the diffraction-specific coherent panoramagram is amenable to a GPU-based implementation.[12] We are in the process of developing a CUDA-based scheme for driving all 18 modulator channels in the Mark IV display to produce a 468-line output in a dynamic fashion and in full color. Methods and results will be detailed in a subsequent publication.

5. CONCLUSIONS

We have described a computational architecture for driving anisotropic leaky-mode modulators as employed for full-color holographic video systems, suitable for handling the input of general (e.g., Fresnel) CGHs to the Mark IV display. Although this approach is computationally expensive, we have furthermore depicted a computationally efficient method for the generation of full-color holographic stereograms via the diffraction-specific coherent panoramagram approach. We anticipate that, when employed in conjunction with GPU-based computational approaches, this approach for generation of full-color holographic stereograms will allow for interactive rate holographic display on the Mark IV system and future displays based around anisotropic leaky-mode modulators.

ACKNOWLEDGMENTS

This work has been supported in part by consortium funding at the MIT Media Laboratory. The authors are grateful to NVIDIA for their generous donation of the GPU hardware used in this work.

REFERENCES

[1] S. A. Benton, "Elements of holographic video imaging," *Society of Photo-Optical Instrumentation Engineers (SPIE) Conference Series*, v. 1600, pp. 8295, 1992.

[2] S. A. Benton and V. M. Bove, Jr., *Holographic Imaging*, Ch. 21. Hoboken, NJ: Wiley, 2008.

[3] T. Senoh, T. Mishina, K. Yamamoto, R. Oi, and T. Kurita, "Wide viewing-zone-angle full-color electronic holography system using very high resolution liquid crystal display panels," *Proc. SPIE Practical Holography XXV: Materials and Applications*, v. 7957, 2011.

[4] D. E. Smalley, Q. Y. J. Smithwick, V. M. Bove, Jr., J. Barabas and S. Jolly, "Anisotropic leaky-mode modulator for holographic video displays," *Nature*, v. 498, pp. 313 - 317, 2013.

[5] A. Matteo, C. Tsai, and N. Do, "Collinear guided wave to leaky wave acoustooptic interactions in proton-exchanged $LiNbO_3$ waveguides," *IEEE Transactions on Ultrasonics, Ferroelectrics and Frequency Control* vol. 47, no. 1, pp. 16-28, 2000.

[6] D. E. Smalley, *Holovideo on a Stick: Integrated Optics for Holographic Video Displays*, Ph.D. thesis, Massachusetts Institute of Technology, 2013.

[7] D. E. Smalley, Q. Y. J. Smithwick, J. Barabas, V. M. Bove, Jr., S. Jolly, and C. Della Silva, "Holovideo for Everyone: a Low-Cost Holovideo Monitor," *J. Phys.: Conf. Ser. 415*, 012055, 2013.

[8] H. W. Lee, "The Scophony Television Receiver," *Nature*, v. 142, 3584, pp. 59-62, 1938.

[9] P. St.-Hilaire, S. A. Benton, M. Lucente, M. L. Jepsen, J. Kollin, and H. Yoshikawa, "Electronic Display System for Computational Holography," *Proc. SPIE Practical Holography IV*, v. 1212, pp. 174-182, 1990.

[10] S. Tretter, "Single Sideband Modulation and Frequency Translation," in *Communication System Design Using DSP Algorithms*, New York: Springer, 2008.

[11] R. N. Bracewell, *The Fourier Transform and Its Applications*, 3rd ed., Ch. 13, New York, NY: McGraw-Hill, 2000.

[12] Q. Y. J. Smithwick, J. Barabas, D. Smalley, and V. M. Bove, Jr., "Interactive Holographic Stereograms with Accommodation Cues," *Proc. SPIE Practical Holography XXIV: Materials and Applications*, 7619, 761903, 2010.

[13] J. Barabas, S. Jolly, D. E. Smalley, and V. M. Bove, Jr., "Diffraction Specific Coherent Panoramagrams of Real Scenes," *Proc. SPIE Practical Holography XXV: Materials and Applications*, v. 7957, 2011.

[14] B. Boashash, "Estimating and interpreting the instantaneous frequency of a signal," *Proceedings of the IEEE*, v. 80, pp. 520-538, 1992.

APPENDIX A: DERIVATION OF SINGLE-SIDEBAND MODULATED CHIRP EQUATION OF WAVEFRONT ELEMENT

The transmittance function of an unmodulated, chirped holographic grating defining a wafel aperture is given as

$$t(x) = \cos\left[\frac{2\pi}{\lambda}\left(\sqrt{(x-x_0)^2+z_0^2} - x_0 + x\sin\theta_r\right)\right] \tag{7}$$

where x is the position on the composite hologram transmittance function, (x_0, z_0) is the position of a scene point to be reconstructed, and θ_r is the angle of the reconstruction beam relative to the normal of the hologram plane.

We derive the single-sideband modulated form of this chirped grating with carrier frequency f_0 from the viewpoint of the analytic signal representation. Given the transmittance function $t(x)$, the analytic signal $t_a(x)$ is given by

$$t_a(x) = t(x) + j\mathcal{H}\{t(x)\} = A(x)e^{j\phi(x)} \tag{8}$$

where $A(x)e^{j\phi(x)}$ is the phasor representation of $t_a(x)$ (comprised of an *instantaneous amplitude* $A(x)$ and *instantaneous phase* $\phi(x)$) and $\mathcal{H}$ denotes Hilbert transformation.[14] We note that this representation allows the Hilbert transform of the signal $t(x)$ to be interpreted as the imaginary part of the phasor $t_a(x)$ and that the relationship

$$\angle t_a(x) = \phi(x) = \tan^{-1}\left(\frac{\mathcal{H}\{t(x)\}}{t(x)}\right) \tag{9}$$

allows for $\mathcal{H}\{t(x)\}$ to be expressed as

$$\mathcal{H}\{t(x)\} = t(x)\tan\phi(x). \tag{10}$$

Noting that the instantaneous phase $\phi(x)$ of $t_a(x)$ is already provided in closed form as

$$\phi(x) = \arg t(x) = \frac{2\pi}{\lambda}\left(\sqrt{(x-x_0)^2+z_0^2} - x_0 + x\sin\theta_r\right), \tag{11}$$

$\mathcal{H}\{t(x)\}$ can be written as

$$\mathcal{H}\{t(x)\} = \cos\left[\frac{2\pi}{\lambda}\left(\sqrt{(x-x_0)^2+z_0^2} - x_0 + x\sin\theta_r\right)\right]\tan\left[\frac{2\pi}{\lambda}\left(\sqrt{(x-x_0)^2+z_0^2} - x_0 + x\sin\theta_r\right)\right]. \tag{12}$$

This reduces to

$$\mathcal{H}\{t(x)\} = \sin\left[\frac{2\pi}{\lambda}\left(\sqrt{(x-x_0)^2+z_0^2} - x_0 + x\sin\theta_r\right)\right]. \tag{13}$$

Given a signal $t(x)$, the single-sideband modulated form $t_{SSB}(x)$ with carrier frequency f_0 is given by

$$t_{SSB}(x) = t(x)\cos(2\pi f_0 x) - \mathcal{H}\{t(x)\}\sin(2\pi f_0 x). \tag{14}$$

Substituting Eqs. (7) and (13) into Eq. (14), we arrive at the relationship

$$\begin{aligned} t_{SSB}(x) = \cos\left[\frac{2\pi}{\lambda}\left(\sqrt{(x-x_0)^2+z_0^2} - x_0 + x\sin\theta_r\right)\right]\cos(2\pi f_0 x) - \\ \sin\left[\frac{2\pi}{\lambda}\left(\sqrt{(x-x_0)^2+z_0^2} - x_0 + x\sin\theta_r\right)\right]\sin(2\pi f_0 x) \end{aligned} \tag{15}$$

which simplifies into the final form of a single-sideband modulated wafel chirp

$$t_{SSB}(x) = \cos\left[\frac{2\pi}{\lambda}\left(\sqrt{(x-x_0)^2+z_0^2} - x_0 + x(\sin\theta_r + \lambda f_0)\right)\right]. \tag{16}$$